

# Recovering the time-dependent transmission rate from infection data

Mark Pollicott<sup>1</sup>, Hao Wang<sup>2†</sup>, and Howie Weiss<sup>3</sup>

<sup>1</sup> *Mathematics Institute, University of Warwick, Coventry, CV4 7AL, United Kingdom*

<sup>2</sup> *Department of Mathematical and Statistical Sciences,*

*University of Alberta, Edmonton, Alberta, T6G 2G1, Canada*

<sup>3</sup> *School of Mathematics, Georgia Institute of Technology, Atlanta, Georgia, 30332, United States\**

(Dated: December 12, 2018)

## Abstract

Background. The transmission rate of many acute infectious diseases varies significantly in time, but the underlying mechanisms are usually uncertain. They may include seasonal changes in the environment, contact rate, immune system response, etc. The transmission rate has been thought impossible to measure directly. We present an algorithm to recover the time-dependent transmission rate directly from prevalence data, which makes no assumptions about the number of susceptibles, vital rates, etc.

Methodology/Principal Findings. The algorithm is derived from the complete and explicit solution of a mathematical inverse problem for SIR-type transmission models. We illustrate the algorithm with the historic (pre-vaccination) UK measles data. Fourier analysis of the recovered transmission rate yields robust spectral peaks with 1- and 1/3-year periods. Many modelers have assumed that measles transmission is entirely driven by school contacts and can be represented by a simple sinusoidal or Haar function with one-year period. Our algorithm also provides a new method to estimate the initial transmission rate via stabilizing the recovered transmission rate function.

Conclusions/Significance. The main objective of this work is to provide a new algorithm to recover the transmission rate function directly from infection data. Our algorithm also yields that almost any infection profile can be perfectly fitted by an SIR-type model with variable transmissibility. This clearly illustrates a serious danger of overfitting an SIR transmission model with time-dependent transmission rate.

---

<sup>†</sup> To whom correspondence should be addressed. Electronic address: hwang@math.ualberta.ca

\*The UK measles data and birth data was obtained from [18] and [9]. The authors very much appreciate the efforts of David Earn and Ben Bolker for maintaining these public databases of infectious disease data. Thank David Earn for helpful discussion.

## I. INTRODUCTION

The transmission rate of an infectious disease is the rate of which susceptible individuals become infected. In Section 3.4.9 of Anderson and May [1], the authors state that “... *the direct measurement of the transmission rate is essentially impossible for most infections. But if we wish to predict the changes wrought by public health programmes, we need to know the transmission rate ...* .” The transmission rate of many acute infectious diseases varies significantly in time and frequently exhibits significant seasonal dependence [3, 12, 36]: influenza, pneumococcus, and rotavirus cases peak in winter; RSV and measles cases peak in spring; and polio cases peak in summer.

Measles outbreaks in several UK cities (pre-vaccination) followed a two-year cycle (see Figure 3(a)(b)), and many investigators have attempted to explain this two-year cycle using mathematical models. Since measles cases, as well as cases of several other childhood viral diseases such as pertussis, seem to strongly correlate with school terms and breaks, most previous modelers have assumed that the measles transmission rate can be represented by a simple sinusoidal [17] or Haar [21] function with one-year period corresponding to the school year. This assumption is based on little empirical evidence and ignores the seasonal changes of the environment, immune system, etc. [16, 28] on the transmission rate. For example, since measles spreads through respiration directly or indirectly through aerosol, the high absolute humidity indoors and outdoors during winter may constrain both transmission efficiency and the virus survival rate [29, 30].

Most investigators estimate the transmission rate of an infectious disease using the formula

$$\beta(k) = \frac{I(k+1)}{I(k)S(k)}, \quad (1)$$

where, for instance,  $S(k), I(k)$  are the fractions of susceptible and infected individuals during week  $k$  [2, 15]. This formula requires knowledge of  $S(k)$ , which is usually very difficult to estimate. Our new algorithm obviates this requirement.

Toward obtaining our new transmission rate recovery algorithm, we first consider the simplest SIR transmission model (Kermack and McKendrick [22]) and allow the transmission rate to be a time-dependent function, *i.e.*, there is a positive function  $\beta(t)$  such that

$$S'(t) = -\beta(t)S(t)I(t), \quad (2)$$

$$I'(t) = \beta(t)S(t)I(t) - \nu I(t), \quad (3)$$

$$R'(t) = \nu I(t), \quad (4)$$

where  $S(t)$ ,  $I(t)$ , and  $R(t)$  are the fractions of susceptible, infected, and removed individuals at time  $t$ . We begin by asking the mathematical question:

*Given smooth infection data on time interval  $[0, T]$  and recovery rate  $\nu > 0$ , can one always choose a transmission rate function  $\beta(t)$  such that the SIR epidemic model always perfectly fits the smooth data with the given  $\nu$ ?*

Mathematicians call this an inverse problem. We prove that this is always possible subject to a mild restriction on the infection data and  $\nu$ , and we provide an explicit formula for the solution. The construction also illustrates the danger of overfitting a transmission model where one can choose the time-dependent transmission rate.

However, in practice, infection data are always discrete, not continuous. We show that one can robustly estimate  $\beta(t)$  by first smoothly interpolating the data with a spline or trigonometric function and then applying the formula to smooth data.

The usual transmission rate recovery method based on (1) can be viewed as a discretization of (3). Our new method not only avoids this crude discretization, but also uses the additional information contained in (2) and (4).

We extend our recovery algorithm to more general classes of transmission models including the SEIR epidemic model with vital rates, and we illustrate the extended algorithm using UK measles data during 1948-1966. To estimate the initial transmission rate  $\beta(0)$ , we numerically examine the upper threshold of  $\beta(0)$  leading to stationary  $\beta(t)$ . When initial transmission rates are larger than this threshold, the recovered transmission rates are non-stationary functions - they exhibit an upward drift. There seems to be no public health or biological explanation for this drift. When initial transmission rates are smaller than this threshold, the recovered transmission rates are stationary functions.

Our recovered transmission rates exhibit two “competing” dominant spectral peaks: at frequencies 1 and 3 per year, respectively. As a consistency check, our recovered  $\beta(t)$  exhibit minima in July-August during the summer school vacation: the months with the fewest number of notifications, and exhibits maxima in January or September during the first month after the winter and summer school vacations: the months with the most number of notifications.

## II. RESULTS

We rigorously derive a mathematical algorithm for recovering the time-dependent transmission rate from infection data. We first apply the algorithm to two simulated data sets representing two

characteristic “types” of infectious diseases. We then illustrate the algorithm using UK measles data from 1948-1966.

### A. Recovery algorithm

Our recovery algorithm is based on a mathematical solution of an inverse problem, which is expanded in Section IV A. To recover the transmission rate  $\beta(t)$  from an infection data set, the recovery algorithm has four steps and requires two conditions.

**Step 1.** Smoothly interpolate the infection data with spline or trigonometric functions to generate a smooth  $f(t)$ . Check condition 1:  $f'(t)/f(t) > -\nu$ , where  $\nu$  is the removal rate.

**Step 2.** Compute the function  $p(t) = \frac{f''(t)f(t) - f'(t)^2}{f(t)(f'(t) + \nu f(t))}$ . Condition 1 prevents a zero denominator in  $p(t)$ .

**Step 3.** Choose  $\beta(0)$  and compute the integral  $P(t) = \int_0^t p(\tau)d\tau$ . Check condition 2:  $\beta(0) < 1 / \int_0^T e^{P(s)} f(s) ds$ , where  $T$  is the time length of the infection data. Alternatively, choose  $\beta(0)$  sufficiently small to satisfy condition 2.

**Step 4.** Apply the formula  $\beta(t) = 1 / \left[ e^{-P(t)}/\beta(0) - e^{-P(t)} \int_0^t e^{P(s)} f(s) ds \right]$  to compute  $\beta(t)$  on the given interval  $[0 T]$ .

Condition 1 is equivalent to  $d(\ln f(t))/dt > -\nu$ , *i.e.*, the time series of infection data cannot decay too fast at any time. This is a mild condition that most data sets satisfy. If a data set does not satisfy this condition, we propose a scaling trick in Section III to be able to apply the algorithm.

In Section IV B, we present extensions of the basic recovery algorithm to several popular extensions of the SIR model, including the SEIR model with variable vital rates. Our algorithm can be extended to virtually any such compartment model.

### B. Recovering the transmission rate from simulated data

We first illustrate the recovery algorithm using two simulated data sets. The functions  $f(t)$  and  $g(t)$  are the fractions of the infected population for two characteristic “types” of infectious diseases.

The first data set simulates an infectious disease with periodic outbreaks, as observed in measles (before mass vaccination) and cholera [5, 26]. The periodic function  $f(t) = 10^{-5}[1.4 + \cos(1.5t)]$  represents the continuous infection data, and Figure 1(a) contains plots of both  $f(t)$  (solid) and its associated transmission rate function  $\beta(t)$  (dashed).

The second data set simulates an infectious disease with periodic outbreaks that decays in time, as observed in influenza [33]. The periodic function  $g(t) = 10^{-5}[1.1 + \sin(t)] \exp(-0.1t)$  represents the continuous infection data, and Figure 2(a) contains plots of both  $g(t)$  (solid) and its associated transmission rate function  $\beta(t)$  (dashed).

We extract discrete data from functions  $f(t)$  and  $g(t)$  by sampling them at equi-spaced intervals (see the small black squares in Figure 1(a) and Figure 2(a)). To each discrete time series, we apply two well-known interpolation algorithms (trigonometric approximation and spline approximation) [23, 35]. Figure 1(b) and Figure 2(b) contain plots of  $\beta(t)$  obtained from the two smooth interpolations together with the recovery algorithm. Both interpolation schemes yield excellent approximations of  $\beta(t)$  in both examples.

Many simulations show that the recovery algorithm is robust with respect to white noise up to 10% of the data mean, as well as the number of sample points.

### C. Recovering the transmission rate from UK measles data

Previous studies [13, 20] employed the SEIR model with vital rates to explore the epidemic and endemic behaviors of measles infections, using the notification data in [27]. To compare our new recovery technique with previous measles studies, we extend our recovery algorithm to the SEIR model with variable vital rates (see Section IV B 5) and use the same data set. To examine the robustness of our new results, we post condition on the data to account for underreporting and reapply the extended recovery algorithm.

We use the measles parameter values from Anderson and May [1], OPCS et al. [27]:  $\nu = 52/\text{year} = 52/12/\text{month}$  (where  $1/\nu$  is the removal period),  $a = 52/\text{year} = 52/12/\text{month}$  (where  $1/a$  is the latent period), and  $\delta = 1/70/\text{year} = 1/70/12/\text{month}$  (death rate, equivalent to the life span of 70 years).

Public databases, such as the International Infectious Disease Data Archive [18] and Bolker's measles data archive [9], contain the weekly numbers of measles notifications from 1948–1966 and the quarterly reported historical UK births from 1948–1956. During 1948–1956 the births show large annual variations (see Figure 3(c)) with a strong 1/year frequency component (see Figure

3(d)). Since some years these variations approach 20%, we include actual births in our model. Since neither database contains the UK birth rates from 1957 – 1966, this requires us to restrict our study to the period 1948 – 1956.

Although disease notification data (the number of reported new infections during a given period) is different from prevalence data (the total number of reported infections during the period), they should be close if the reporting period is longer than the mean generation time of infection. Previous measles modelers have used notification data as a surrogate for the number of infected individuals [13, 38]. To be able to compare our results with those of previous authors, we first apply our recovery algorithm to the same notification data and then check the robustness of our algorithm by applying it to estimated prevalence data. We thank David Earn for clarifying these issues for us.

Since the birth data is provided only quarterly and the notifications weekly, we smoothly interpolate the birth data and aggregate the notification data into one month intervals. To aggregate weekly infection data into monthly data, we simply sum the weekly data as previous studies [13, 38]. For a week across two months, this weekly infection number is separated to be two parts. For instance, if one week has three days in May and four days in June, then we multiply the notification data of this week by  $3/7$  and incorporate it into May data, and we multiply the notification data of this week by  $4/7$  and incorporate it into June data.

Previous authors represented the time-varying transmission rate using a sinusoidal or Haar function, and fitted parameters using the method of least squares, without providing variances for their estimates [8]. Little empirical evidence can support their assumed functions. The school mixing assumption behind these simple transmission functions ignores many other seasonal factors such as environmental changes and immune system changes [16, 28]. The transmission rate has a huge variation as tested numerically and assumed in previous studies [6, 13, 14, 20]. Even the ballpark range of the transmission rate function is highly uncertain [24, 38], in part since it depends on guessing the size of susceptible population.

Our recovery algorithm provides a robust new way of estimating  $\beta(0)$ . The idea is to select the largest value of  $\beta(0)$  such that the recovered time series  $\beta(t)$  is stationary. For measles, the upper threshold of stationary  $\beta(0)$  lies between 140 and 150. If one assumes that the probability of measles transmission during an effective contact is 5% [4], then this range of  $\beta(0)$  corresponds to an infected child having an average of about eight adequate contacts per day during January. Other authors have assumed that  $\beta(0) = 1299$  (the averaged transmission rate in January computed from their term-based step function where  $\beta = 846$  during January 1-6 and  $\beta = 1408$  during January

7-31) [20, 21], which corresponds to an infected child having about 70 adequate contacts per day. Early January is during the school winter break when children have far fewer contacts than during the school year. Presumably most of the infected kids stayed home once they knew they were infected [7, 32, 34], and there appears to be few asymptomatic cases in children [31], thus we believe that the lower estimate of daily contacts provided by our algorithm seems more plausible.

In Figure 4(a)(c)(e)(g), we plot the transmission rates  $\beta(t)$  recovered from our algorithm for four different January initial values chosen to represent a wide range of  $\beta(0)$ . The recovered  $\beta(t)$  in panels (e)(g) are stationary, slowly increasing peaks in panel (c), and fast increasing peaks in panel (a). Note that annual minima occur in July-August during the summer school vacation period and that annual maxima occur in January or September during the first month after the winter and summer school vacations.

In Figure 4(b)(d)(f)(h), we plot the moduli of Fourier transform of all recovered  $\beta(t)$  and observe that there are two competing dominant spectral peaks. These two dominant peaks have 1 and 1/3-year periods. The source of the three per year (*i.e.*, 1/3-year period) peak of  $\beta(t)$  remains mysterious and does not occur in the notification time series. For stationary  $\beta(t)$  (see panels (e)(g)), the one per year spectral peak is dominant (see panels (f)(h)), and the one half per year (*i.e.*, 2-year period) spectral peak is comparable to the three per year spectral peak (see panel (h)). Clearly our recovered transmission rates are much more complex functions than pure sinusoidal or Haar function with one year period.

To test the robustness of our spectral peaks, we incorporate the standard correction factor of 92.3% to account for the underreporting bias in the UK measles data (with estimated mean reporting rate 52%, note that 92.3% is computed from  $1/0.52 - 1$ ) [6, 10, 37]. Since both the removal stage in the SEIR model and the data notification period are one week, and the 92.3% correction factor essentially doubles the number of cases, this corrected number of cases will account for the non-notified cases during this removal stage. Hence, the corrected weekly notification data should provide a good approximation for total weekly infections. This precise methodology was used in [6, 8].

We plot the recovered  $\beta(t)$  with the 92.3% correction factor and for the large range of  $\beta(0)$  in Figure 5. All the recovered  $\beta(t)$  have identical spectral peaks as those in Figure 4. Thus our observation of the two spectral peaks with frequencies 1/year and 3/year seems robust. The scale of the infection data regulates the scale of  $\beta(t)$  but does not affect spectral peaks of Fourier transform of  $\beta(t)$ .

### III. DISCUSSION

In this paper, we provide a new algorithm to recover the time-dependent transmission rate from infection data. The algorithm only requires the number of infected individuals during each time interval, and does not require the number of susceptible individuals, as does the commonly used method.

We illustrate the recovery algorithm for the SEIR model with variable vital rates using UK measles data from 1948 to 1956. Fourier transform of our recovered transmission rate function shows dominant spectral peaks at frequencies 1 and 3 per year. All previous measles transmission models assumed a one-year periodic transmission rate function to account for mixing of children in school, which seems reasonable for the stationary case. However, they neglect the large three times per year cycle which can be dominant in transmission rates with fast increasing peaks. This can have profound consequences for the dynamics of the system of nonlinear ODEs. In addition, our recovery algorithm provides a robust new method to estimate  $\beta(0)$  which does not involve guestimating  $S(0)$ , and we believe that the estimate provided by our algorithm seems more plausible than existing estimates.

Our algorithm has some limitations to its applicability. First, the proportion of infected individuals,  $f(t)$ , can not decrease too fast over the full time interval of interest. In general, one can add a sufficiently large constant to  $f(t)$  to ensure this, but this will change the range of applicable  $\beta(0)$ , and applicability needs to be checked. Second, one must assume that the proportion (or number) of notifications is always strictly positive. In practice this restriction can be overcome by replacing zero values in the time series with a very small positive value. Third, for a chosen  $\beta(0)$ , the algorithm can only apply to a finite length of infection data. Finally, one either needs to know the value of the transmission rate at some fixed time, or verify that the desired properties of  $\beta(t)$  hold for all  $\beta(0)$  in the range where the estimated  $\beta(t)$  is stationary.

The algorithm should apply to the vast majority of infection data sets, and a consequence is that one can nearly always construct a time-dependent transmission rate  $\beta(t)$  such that SIR model will fit the data perfectly. This illustrates a potential danger of overfitting an epidemic model with time-dependent transmission rate.



## IV. MATERIALS AND METHODS

### A. Mathematical derivation

The recovery algorithm follows from the following complete solution of the inverse problem.

**Theorem IV.1** *Given a smooth positive function  $f(t)$ ,  $\nu > 0$ , and  $T > 0$ , there exists  $K > 0$  such that if  $\beta(0) < K$  there is a solution  $\beta(t)$  with  $\beta(0) = \beta_0$  such that  $I(t) = f(t)$  for  $0 \leq t \leq T$  if and only if  $f'(t)/f(t) > -\nu$  for  $0 \leq t \leq T$ .*

The growth condition imposes no restrictions on how  $f(t)$  increases, but requires that  $f(t)$  cannot decrease too quickly, in the sense that its logarithmic derivative is always bounded below by  $-\nu$ . It is easy to see that  $f'(t)/f(t) > -\nu$  is a necessary condition, since Equation (3) implies that  $f'(t) + \nu f(t) = \beta(t)S(t)f(t)$ , which must be positive for  $0 \leq t \leq T$ .

The proof of the theorem consists of showing that this condition is also sufficient. We rewrite Equation (3) as

$$S(t) = \frac{f'(t) + \nu f(t)}{\beta(t)f(t)}, \quad (5)$$

then compute  $S'(t)$ , and then equate with Equation (2) to obtain

$$\frac{d}{dt} \left( \frac{f'(t) + \nu f(t)}{\beta(t)f(t)} \right) = -\beta(t) \left( \frac{f'(t) + \nu f(t)}{\beta(t)f(t)} \right) f(t). \quad (6)$$

Calculating the derivative and simplifying the resulting expression yields the following Bernoulli differential equation for  $\beta(t)$

$$\beta'(t) - p(t)\beta(t) - f(t)\beta^2(t) = 0, \quad \text{where} \quad p(t) = \frac{f''(t)f(t) - f'(t)^2}{f(t)(f'(t) + \nu f(t))}. \quad (7)$$

The change of coordinates  $x(t) = 1/\beta(t)$  transforms this nonlinear ODE into the linear ODE

$$x'(t) - p(t)x(t) - f(t) = 0. \quad (8)$$

The method of integrating factors provides the explicit solution

$$\frac{1}{\beta(t)} = x(t) = x(0)e^{-P(t)} - e^{-P(t)} \int_0^t e^{P(s)} f(s) ds, \quad \text{where} \quad P(t) = \int_0^t p(\tau) d\tau. \quad (9)$$

A problem that could arise with this procedure is for the denominator of  $p(t)$  to be zero. A singular solution is prevented by requiring that the denominator be always positive, *i.e.*,  $f'(t) + \nu f(t) > 0$ . Having done this, to ensure that  $\beta(t)$  is positive,  $\beta(0)$  must satisfy

$$\int_0^T e^{P(s)} f(s) ds < 1/\beta(0). \quad (10)$$

Mathematically, there are infinitely many choices of  $\beta(0)$  and thus infinitely many transmission functions  $\beta(t)$ . In this sense the inverse problem is under-determined. This observation clearly illustrates a serious danger of overfitting such an epidemic transmission model.

## B. Extensions of the basic model

Analogous results and inversion formulae hold for all standard variations of the standard SIR model and their combinations. The proofs are very similar to the proof of Theorem (IV.1). Here, we only present the full algorithm for the SEIR model with vital rates, since we apply this algorithm to UK measles data.

### 1. SIR model with vital rates

$$S'(t) = \delta - \beta(t)S(t)I(t) - \delta S(t), \quad (11)$$

$$I'(t) = \beta(t)S(t)I(t) - \nu I(t) - \delta I(t), \quad (12)$$

$$R'(t) = \nu I(t) - \delta R(t). \quad (13)$$

The necessary and sufficient condition for recovering  $\beta(t)$  given  $\nu$  and  $\delta$  is  $f'(t)/f(t) > -(\nu + \delta)$ .

### 2. SIR model with waning immunity

$$S'(t) = mR(t) - \beta(t)S(t)I(t), \quad (14)$$

$$I'(t) = \beta(t)S(t)I(t) - \nu I(t), \quad (15)$$

$$R'(t) = \nu I(t) - mR(t), \quad (16)$$

where  $1/m$  is the memory period of immunity. The necessary and sufficient condition for recovering  $\beta(t)$  given  $\nu$  is  $f'(t)/f(t) > -\nu$ .

### 3. SIR model with time-dependent indirect transmission rate (Joh et al. [19])

$$S'(t) = -\omega(t)S(t), \quad (17)$$

$$I'(t) = \omega(t)S(t) - \nu I(t), \quad (18)$$

$$R'(t) = \nu I(t), \quad (19)$$

where  $\omega(t)$  is the time-dependent indirect transmission rate. The necessary and sufficient condition for recovering  $\beta(t)$  given  $\nu$  is  $f'(t)/f(t) > -\nu$ .

## 4. SEIR model

$$S'(t) = -\beta(t)S(t)I(t), \quad (20)$$

$$E'(t) = \beta(t)S(t)I(t) - \alpha E(t), \quad (21)$$

$$I'(t) = \alpha E(t) - \nu I(t), \quad (22)$$

$$R'(t) = \nu I(t), \quad (23)$$

where  $1/\alpha$  is the latent period for the disease. By simple calculations, we can show that the necessary and sufficient condition for recovering  $\beta(t)$  from infection data is  $f'(t)/f(t) > -\nu$ .

## 5. SEIR model with vital rates

$$S'(t) = \delta - \beta(t)S(t)I(t) - \delta S(t), \quad (24)$$

$$E'(t) = \beta(t)S(t)I(t) - aE(t) - \delta E(t), \quad (25)$$

$$I'(t) = aE(t) - \nu I(t) - \delta I(t), \quad (26)$$

$$R'(t) = \nu I(t) - \delta R(t). \quad (27)$$

The necessary and sufficient conditions for recovering  $\beta(t)$  from infection data are

$$f'(t) + (\nu + \delta)f(t) > 0 \quad \text{and} \quad f''(t) + (\nu + 2\delta + a)f'(t) + (\delta + a)(\nu + \delta)f(t) > 0. \quad (28)$$

In this case,  $\beta(t)$  satisfies the Bernoulli equation

$$\beta' + p(t)\beta + q(t)\beta^2 = 0, \quad (29)$$

where

$$p(t) = \frac{-af'''(t)f(t) - a(\nu + 2\delta + a)f''(t)f(t) - a(\delta + a)(\nu + \delta)f'(t)f(t) + af''(t)f'(t) + a(\nu + 2\delta + a)f'(t)^2}{af(t)[f''(t) + (\nu + 2\delta + a)f'(t) + (\delta + a)(\nu + \delta)f(t)]} + \frac{a(\delta + a)(\nu + \delta)f'(t)f(t) - \delta af''(t)f(t) - \delta a(\nu + 2\delta + a)f'(t)f(t) - \delta a(\delta + a)(\nu + \delta)f^2(t)}{af(t)[f''(t) + (\nu + 2\delta + a)f'(t) + (\delta + a)(\nu + \delta)f(t)]},$$

and

$$q(t) = \frac{\delta a^2 f^2(t) - af''(t)f^2(t) - a(\nu + 2\delta + a)f'(t)f^2(t) - a(\delta + a)(\nu + \delta)f^3(t)}{af(t)[f''(t) + (\nu + 2\delta + a)f'(t) + (\delta + a)(\nu + \delta)f(t)]}.$$

The modified recovery algorithm has five steps together with three conditions.

**Step 1.** Smoothly interpolate the infection data to generate a smooth function  $f(t)$  that has at least a continuous second derivative. Check condition 1:  $f'(t) + (\nu + \delta)f(t) > 0$ ; and check condition 2:  $f''(t) + (\nu + 2\delta + a)f'(t) + (\delta + a)(\nu + \delta)f(t) > 0$ .

**Step 2.** Compute the function  $p(t) = \frac{-af'''(t)f(t) - a(\nu + 2\delta + a)f''(t)f(t) - a(\delta + a)(\nu + \delta)f'(t)f(t) + af''(t)f'(t) + a(\nu + 2\delta + a)f'(t)^2}{af(t)[f''(t) + (\nu + 2\delta + a)f'(t) + (\delta + a)(\nu + \delta)f(t)]} + \frac{a(\delta + a)(\nu + \delta)f'(t)f(t) - \delta af''(t)f(t) - \delta a(\nu + 2\delta + a)f'(t)f(t) - \delta a(\delta + a)(\nu + \delta)f^2(t)}{af(t)[f''(t) + (\nu + 2\delta + a)f'(t) + (\delta + a)(\nu + \delta)f(t)]}$ .

**Step 3.** Choose  $\beta(0)$  and compute the integral  $P(t) = \int_0^t p(\tau) d\tau$ . Check condition 3:

$$\frac{1}{\beta(0)} + \int_0^T e^{-P(s)} q(s) ds > 0.$$

**Step 4.** Compute the function  $q(t) = \frac{\delta a^2 f^2(t) - af''(t)f^2(t) - a(\nu + 2\delta + a)f'(t)f^2(t) - a(\delta + a)(\nu + \delta)f^3(t)}{af(t)[f''(t) + (\nu + 2\delta + a)f'(t) + (\delta + a)(\nu + \delta)f(t)]}$ .

**Step 5.** Apply the formula  $\beta(t) = 1 \left/ \left[ e^{P(t)} / \beta(0) + e^{P(t)} \int_0^t e^{-P(s)} q(s) ds \right] \right.$  to compute  $\beta(t)$  on the given interval  $[0, T]$ .

With variable birth rate  $\eta(t)$  and constant death rate  $\delta$ , then the SEIR model becomes

$$S'(t) = \eta(t) - \beta(t)S(t)I(t) - \delta S(t), \quad (30)$$

$$E'(t) = \beta(t)S(t)I(t) - aE(t) - \delta E(t), \quad (31)$$

$$I'(t) = aE(t) - \nu I(t) - \delta I(t), \quad (32)$$

$$R'(t) = \nu I(t) - \delta R(t). \quad (33)$$

In this case, the formula in Step 4 should be

$$q(t) = \frac{\eta(t)a^2 f^2(t) - af''(t)f^2(t) - a(\nu + 2\delta + a)f'(t)f^2(t) - a(\delta + a)(\nu + \delta)f^3(t)}{af(t)[f''(t) + (\nu + 2\delta + a)f'(t) + (\delta + a)(\nu + \delta)f(t)]}.$$

All other steps in the algorithm remain the same.

- 
- [1] Anderson RM, May RM (1992) Infectious Diseases of Humans: Dynamics and Control. Oxford University Press.
  - [2] Becker NG (1989) Analysis of infectious disease data. Chapman and Hall Ltd, New York.
  - [3] Becker NG, Britton T (1999) Statistical studies of infectious disease incidence. Journal of the Royal Statistical Society: Series B (Statistical Methodology) 61: 287-307.
  - [4] Beggs CB, Shepherd SJ, Kerr KG (2010) Potential for airborne transmission of infection in the waiting areas of healthcare premises: stochastic analysis using a Monte Carlo model. BMC Infectious Diseases 10: 247-254.
  - [5] Sanitary Commissioner for Bengal Reports and Bengal Public Health Reports (1891-1942) Bengal Secretariat Press, Calcutta and Bengal Government Press, Alipore.

- [6] Bjørnstad ON, Finkenstädt BF, Grenfell BT (2002) Dynamics of measles epidemics: estimating scaling of transmission rates using a time series SIR model. *Ecological Monographs* 72: 169-184.
- [7] Anonymous (1947) Day Nurseries and Industry. *British Medical Journal* 1: 644-645.
- [8] Bolker BM, Grenfell BT (1993) Chaos and Biological Complexity in Measles Dynamics. *Proc. R. Soc. Lond. B* 251: 75-81.
- [9] Infectious disease data, <http://people.biology.ufl.edu/bolker/measdata.html>.
- [10] Clarkson JA, Fine PEM (1985) The Efficiency of Measles and Pertussis Notification in England and Wales. *International Journal of Epidemiology* 14: 153-168.
- [11] Codeço CT (2001) Endemic and epidemic dynamics of cholera: the role of the aquatic reservoir. *BMC Infect Dis* 1: 1.
- [12] Dowell SF (2001) Seasonal Variation in Host Susceptibility and Cycles of Certain Infectious Diseases. *Emerging Infectious Diseases* 7.
- [13] Earn DJD, Rohani P, Bolker BM, Grenfell BT (2000) A Simple Model for Complex Dynamical Transitions in Epidemics. *Science* 287: 667-670.
- [14] Ellner SP, Bailey BA, Bobashev GV, Gallant AR, Grenfell BT, Nychka DW (1998) Noise and Nonlinearity in Measles Epidemics: Combining Mechanistic and Statistical Approaches to Population Modeling. *The American Naturalist* 151: 425-440.
- [15] Fine PEM, Clarkson JA (1982) Measles in England and Wales - I: An Analysis of Factors Underlying Seasonal Patterns. *International Journal of Epidemiology* 11: 5-14.
- [16] Fujinami RS, Sun X, Howell JM, Jenkin JC, Burns JB (1998) Modulation of Immune System Function by Measles Virus Infection: Role of Soluble Factor and Direct Infection. *Journal of Virology* 72: 9421-9427.
- [17] Grassly NC, Fraser C (2006) Seasonal infectious disease epidemiology. *Proc Roy Soc B: Biological Science* 273: 2541-2550.
- [18] International Infectious Disease Data Archive, <http://iidda.mcmaster.ca/>.
- [19] Joh RI, Wang H, Weiss H, Weitz JS (2009) Dynamics of indirectly transmitted infectious diseases with immunological threshold. *Bulletin of Mathematical Biology* 71: 845-862.
- [20] Keeling MJ, Rohani R (2008) Modeling infectious diseases in humans and animals. Princeton University Press.
- [21] Keeling MJ, Rohani P, Grenfell BT (2001) Seasonally forced disease dynamics explored as switching between attractors. *Physica D* 148: 317-335.
- [22] Kermack WO, McKendrick AG (1927) A contribution to the mathematical theory of epidemics. *Proc Roy Soc Lond A* 115: 700-721.
- [23] Kincaid D, Cheney W (2002) Numerical analysis: mathematics of scientific computing (3rd edition). American Mathematical Society, 788 pages.
- [24] London WP, Yorke JA (1973) Recurrent outbreaks of measles, chickpox and mumps I. Seasonal variation in contact rates. *American Journal of Epidemiology* 98: 453-468.

- [25] Markowitz LE, Preblud SR, Fine PE, Orenstein WA (1990) Duration of live measles vaccine-induced immunity. *Pediatr Infect Dis J* 9: 101-110.
- [26] Mollison D (1995) *Epidemic Models: Their Structure and Relation to Data*. Cambridge University Press.
- [27] The weekly OPCS (Office of Population Censuses and Surveys) reports, the Registrar General's Quarterly or Annual Reports, & various English census reports.
- [28] Patz JA, Graczyk TK, Geller N, Vittor AY (2000) Effects of environmental change on emerging parasitic diseases. *International Journal for Parasitology* 30: 1395-1405.
- [29] Remington PL, Hall WN, Davis IH, Herald A, Gunn R (1985) Airborne Transmission of Measles in a Physician's Office. *The Journal of the American Medical Association* 253: 1574-1577.
- [30] Shaman J, Kohn M (2009) Absolute humidity modulates influenza survival, transmission, and seasonality. *PNAS* 106: 3243-3248.
- [31] van den Hof S, Meffre CM, Conyn-van Spaendonck MA, Woonink F, de Melker HE, van Binnendijk RS (2001) Measles outbreak in a community with very low vaccine coverage, the Netherlands. *Emerg Infect Dis.* 7: 593-597.
- [32] [http://www.whale.to/v/measles\\_deaths.html](http://www.whale.to/v/measles_deaths.html) (2008) Measles deaths quotes.
- [33] WHO/NREVSS regional reports published in the CDC's Influenza Summary Update (2001).
- [34] Wichmann O, Siedler A, Sagebiel D, Hellenbrand W, Santibanez S, Mankertz A, Vogt G, Treeck U, Krause G (2009) Further efforts needed to achieve measles elimination in Germany: results of an outbreak investigation. *Bull World Health Organ* 87: 108-115.
- [35] Wolfram Mathematica Documentation Center.
- [36] Wolkewitz M, Dettenkofer M, Bertz H, Schumacher M, Huebner J (2008) Statistical epidemic modeling with hospital outbreak data. *Stat. Med.* 27: 6522-6531.
- [37] Xia Y, Bjørnstad ON, Grenfell BT (2004) Measles Metapopulation Dynamics: A Gravity Model for Epidemiological Coupling and Dynamics. *American Naturalist* 164: 267-281.
- [38] Yorke JA, London WP (1973) Recurrent outbreaks of measles, chickenpox and mumps II. Systematic differences in contact rates and stochastic effects. *American Journal of Epidemiology* 98: 469-482.

Figure 1. (a) We extract 21 equally spaced data points from the periodic function  $f(t) = 10^{-5}[1.4 + \cos(1.5t)]$ ; the dashed curve is  $\beta(t)$  recovered from  $f(t)$  using (9). (b) These transmission functions are estimated using spline and trigonometric interpolations on the 21 data points.

Figure 2. (a) We extract 21 equally spaced data points from the oscillatory decaying function  $g(t) = 10^{-5}[1.1 + \sin(t)] \exp(-0.1t)$ ; the dashed curve is  $\beta(t)$  recovered from  $g(t)$  using (9). (b) These transmission functions are estimated using spline and trigonometric interpolations on the 21 data points.

Figure 3. (a) Aggregated monthly measles data from England and Wales in 1948 – 1956. (b) Fourier transform of filtered and smoothly interpolated aggregated monthly data showing the dominant frequency components (normalized modulus). Note: we filter and remove the artificial peak at zero frequency in Fourier transform. (c) UK birth rates during 1948 – 1956. (d) Fourier transform of smoothly interpolated UK birth data showing the dominant frequency component (normalized modulus).

Figure 4. The transmission rate function  $\beta(t)$  recovered from our extended algorithm with historic birth rates. (a) The recovered  $\beta(t)$  with  $\beta(0) = 270$ : fast increasing peaks. (b) Fourier transform of filtered  $\beta(t)$  showing the dominant frequency component, 3 per year. (c) The recovered  $\beta(t)$  with  $\beta(0) = 230$ : slowly increasing peaks. (d) Fourier transform of filtered  $\beta(t)$  showing two comparable dominant frequencies components, 1 and 3 per year. (e) The recovered  $\beta(t)$  with  $\beta(0) = 140$ : stationary peaks. (f) Fourier transform of filtered  $\beta(t)$  showing the dominant frequency component, 1 per year. (g) The recovered  $\beta(t)$  with  $\beta(0) = 80$ : stationary peaks. (h) Fourier transform of filtered  $\beta(t)$  showing the dominant frequency component, 1 per year; 1/2 per year peak is large and comparable to 3 per year peak.

Figure 5. We test our estimations of  $\beta(t)$  with data correction. The moduli of Fourier transform of  $\beta(t)$  with the 92.3% correction factor have identical spectral peaks as those without data correction in Figure 4. (a) The recovered  $\beta(t)$  with  $\beta(0) = 120$ . (c) The recovered  $\beta(t)$  with  $\beta(0) = 100$ . (e) The recovered  $\beta(t)$  with  $\beta(0) = 60$ . (g) The recovered  $\beta(t)$  with  $\beta(0) = 30$ . Panels (b)(d)(f)(h) plot moduli of Fourier transform of corresponding  $\beta(t)$  in (a)(c)(e)(g), respectively.

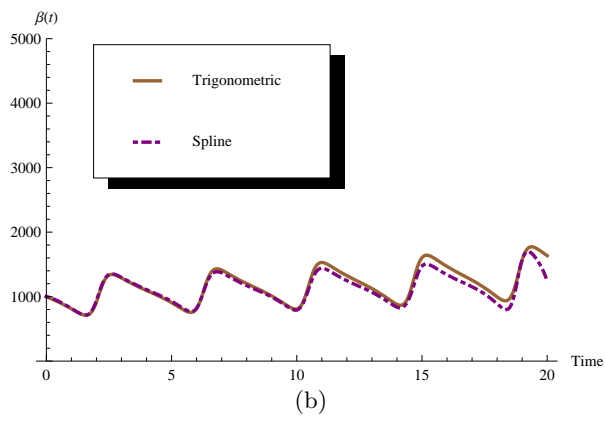
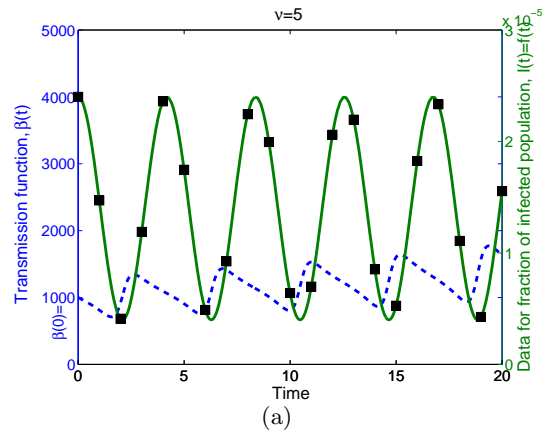


FIG. 1:



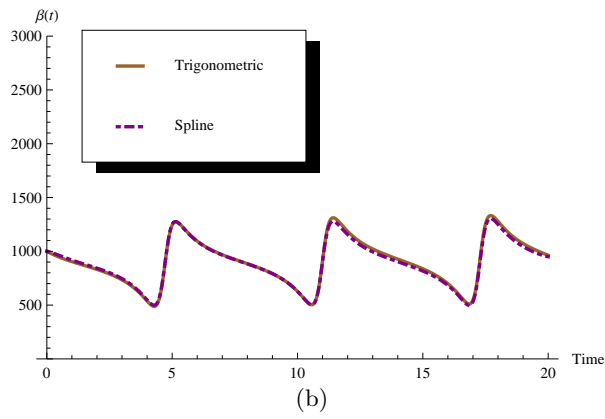
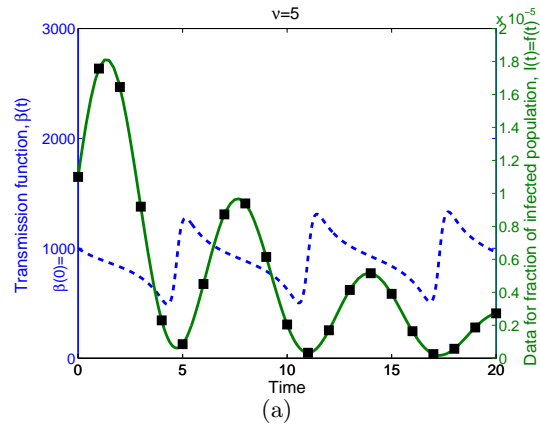


FIG. 2:

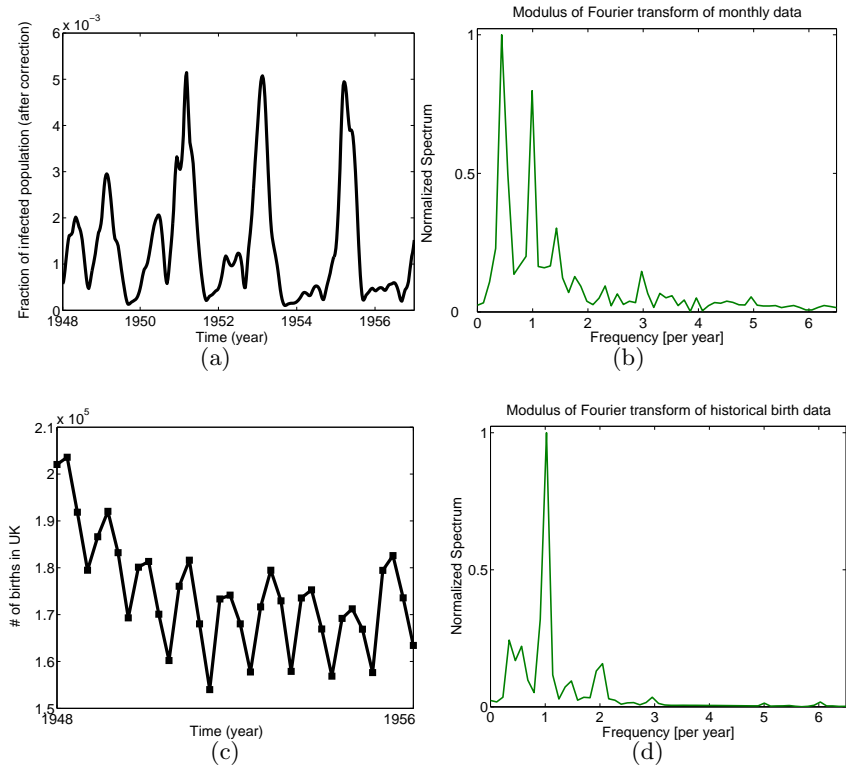


FIG. 3:

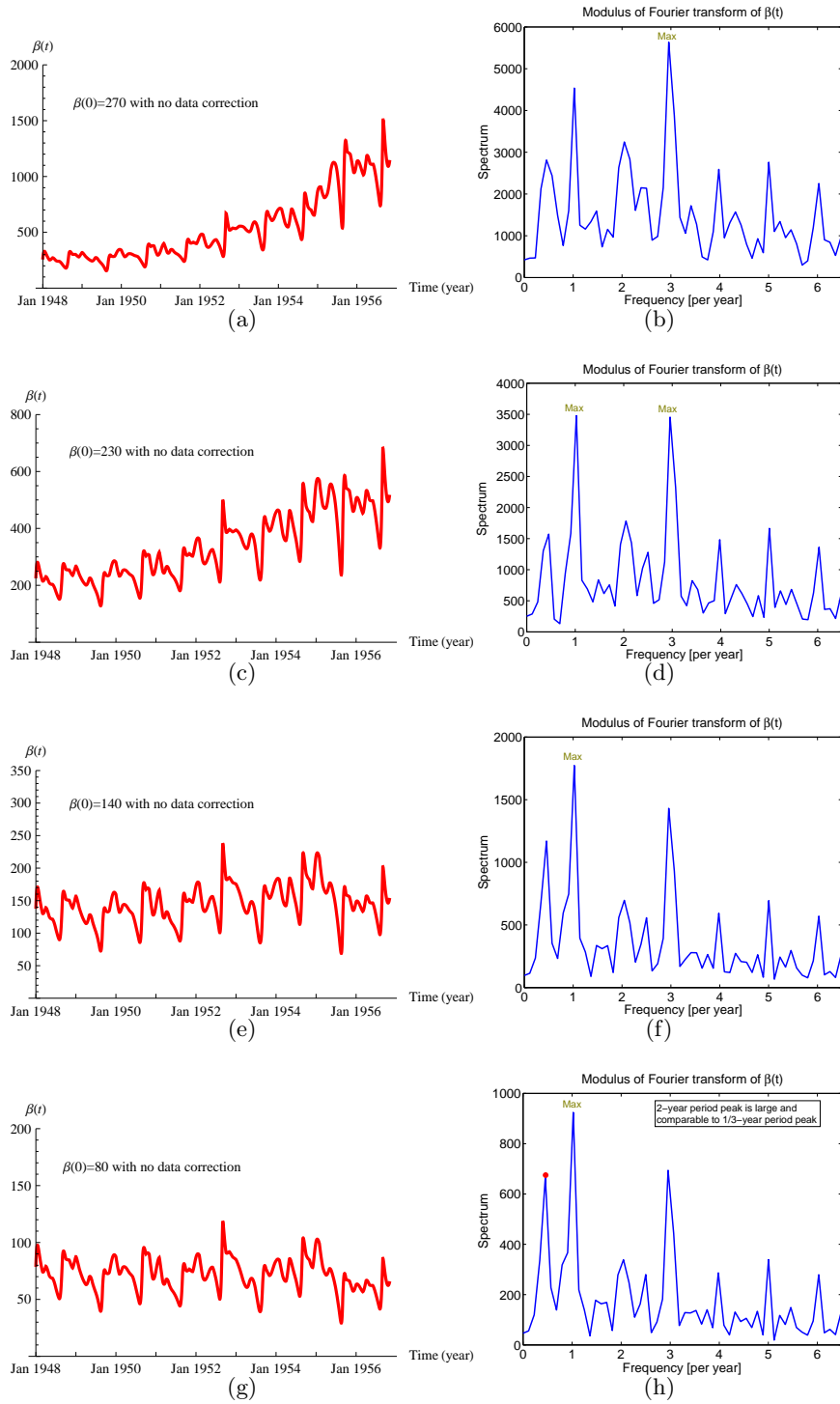


FIG. 4:

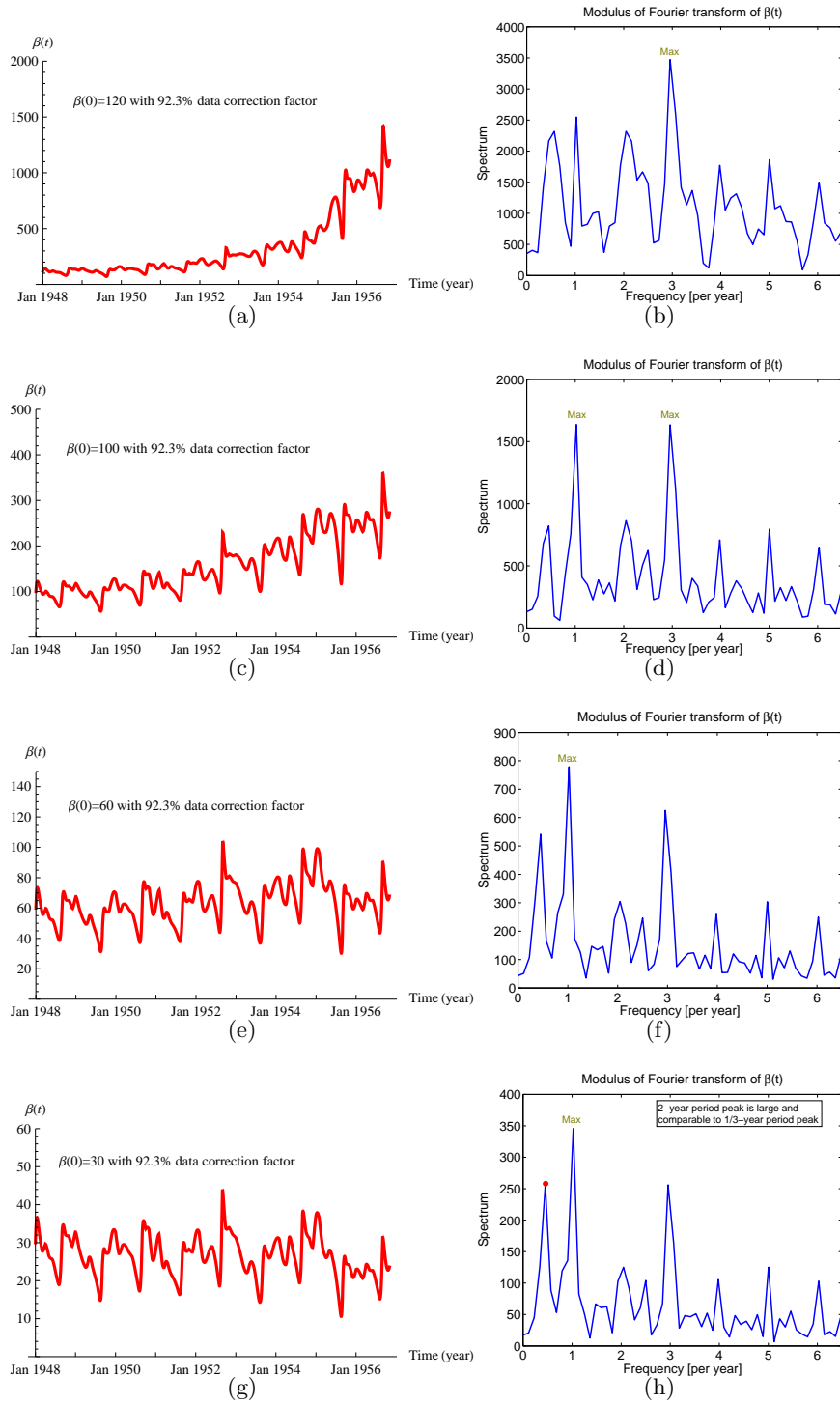


FIG. 5: